Published OnlineFirst February 8, 2011; DOI: 10.1158/0008-5472.CAN-10-2422

Noncytotoxic Differentiation Treatment of Renal Cell Cancer

Soledad Negrotto[1], Zhenbo Hu[1], Oscar Alcazar[1], Kwok Peng Ng[1], Pierre Triozzi[1,2,3], Daniel Lindner[1], Brian Rini[1,3], and Yogen Saunthararajah[1,2]

Abstract

Current drug therapy for metastatic renal cell cancer (RCC) results in temporary disease control but not cure, necessitating continued investigation into alternative mechanistic approaches. Drugs that inhibit chromatin-modifying enzymes involved in transcription repression (chromatin-relaxing drugs) could have a role, by inducing apoptosis and/or through differentiation pathways. At low doses, the cytosine analogue decitabine (DAC) can be used to deplete DNA methyl-transferase 1 (DNMT1), modify chromatin, and alter differentiation without causing apoptosis (cytotoxicity). Noncytotoxic regimens of DAC were evaluated for *in vitro* and *in vivo* efficacy against RCC cell lines, including a p53-mutated RCC cell line developed from a patient with treatment-refractory metastatic RCC. The cell division–permissive mechanism of action—absence of early apoptosis or DNA damage, increase in expression of HNF4α (hepatocyte nuclear factor 4α), a key driver associated with the mesenchymal to epithelial transition, decrease in mesenchymal marker expression, increase in epithelial marker expression, and late increase in cyclin-dependent kinase inhibitor CDKN1B (p27) protein—was consistent with differentiation-mediated cell-cycle exit. *In vivo* blood counts and animal weights were consistent with minimal toxicity of therapy. The distinctive mechanism of action of a dose and schedule of DAC designed for noncytotoxic depletion of DNMT1 suggests a potential role in treating RCC. *Cancer Res; 71(4); 1431–41. ©2011 AACR.*

Introduction

Therapy targeted at VEGF and mTOR pathways now represents the standard of care in metastatic renal cell cancer (RCC; reviewed in ref. 1). Typically, resistance develops to treatment after 6 to 15 months (1). Although the mechanisms by which VEGF and mTOR pathway inhibitors produce temporary disease control are not completely understood, these agents may exercise much of their antitumor activity by antagonizing HIF-1α–mediated proangiogenic effects (1). Drugs with a different mechanism of action could complement these existing therapies to extend the period of disease control.

Agents that inhibit chromatin-modifying enzymes involved in transcription repression (chromatin-relaxing drugs) could have a role in treating RCC (2–4; reviewed in ref. 5). A number of downstream pathways have been implicated in mediating the anti-RCC effects of these drugs (2–5). Broadly speaking, the antiproliferative effect could be mediated by apoptosis pathways and/or by differentiation pathways. Effects of some classes of chromatin-relaxing drugs such as histone deacetylase inhibitors that are not restricted to inhibition of chromatin-modifying enzymes have been suggested to mediate antitumor effects by both apoptotic and differentiation pathways. Although the cytosine analogue decitabine (DAC), which depletes DNA methyl-transferase 1 (DNMT1), can also cause both apoptosis and alter differentiation (6) at low doses, DAC can be used to modify chromatin (7) and alter differentiation without cytotoxicity (8–11). However, DAC has not been evaluated *in vitro* and *in vivo* against RCC at a dose and schedule designed and verified for noncytotoxic DNMT1 depletion, even though the ability of DAC to activate expression of various methylated or immune-related genes in RCC cells has been evaluated (2–4, 12). Furthermore, the possible role of mesenchymal to epithelial differentiation in mediating cell-cycle exit in response to DAC treatment has not been studied. Reasons for evaluating a noncytotoxic DAC regimen in RCC include the likelihood of less toxicity to normal stem cells (low concentrations of DAC increase normal hematopoietic stem cell self-renewal; refs. 13–16), which could facilitate increased exposure to therapy (an important consideration with this S-phase-specific agent), and differentiation–mediated cell-cycle exit, which could be p53-independent and mechanistically distinct from existing therapy (the p53 pathway is frequently suppressed in malignant cells, including renal cancer cells; refs. 17, 18).

Therefore, noncytotoxic regimens of DAC were evaluated for *in vitro* and *in vivo* effects in normal kidney epithelial cells

Authors' Affiliations: [1]Department of Translational Hematology and Oncology Research; [2]Department of Hematologic Oncology and Blood Disorders; and [3]Department of Solid Tumor Oncology, Taussig Cancer Institute, Cleveland Clinic, Cleveland, Ohio

Note: Supplementary data for this article are available at Cancer Research Online (http://cancerres.aacrjournals.org/).

S. Negrotto, Z. Hu, and O. Alcazar contributed equally to the work.

Corresponding Author: Yogen Saunthararajah, Taussig Cancer Institute, 9500 Euclid Avenue R40, Cleveland, OH 44195. Phone: 216-444-8170; Fax: 216-636-2498; E-mail: saunthy@ccf.org

doi: 10.1158/0008-5472.CAN-10-2422

©2011 American Association for Cancer Research.

Downloaded from cancerres.aacrjournals.org on July 24, 2018. © 2011 American Association for Cancer Research.

Published OnlineFirst February 8, 2011; DOI: 10.1158/0008-5472.CAN-10-2422

and RCC cell lines, including a *TP53*-mutated RCC cell line developed from a patient with treatment refractory metastatic RCC. The expression of genes and proteins was examined in the treated cells to understand the pathway and mechanism for cell-cycle exit and to distinguish between apoptosis- and differentiation-based mechanisms. Blood counts and animal weights were used to assess toxicity of *in vivo* therapy. The results and mechanism of action information from these studies provide support for a mechanistically distinct approach to RCC therapy.

Materials and Methods

Derivation and culture of the Ren-01 cell line

A 2-mm diameter biopsy sample from a patient with sunitinib- and bevacizumab-resistant metastatic RCC was implanted subcutaneously into the flank of an athymic nu/nu mouse. Over 4 weeks, the tumor grew to 10-mm diameter. The tumor was passaged serially into 2 additional mice. Tumor cells were dissociated *in vitro*, and a cell line (Ren-01) was established. The line could be cryopreserved and thawed and remained tumorigenic. Ren-01 were cultured in Iscove's modified Dulbecco's medium supplemented with 10% FBS and antibiotics (penicillin/streptomycin), initially seeding 1×10^5 cells per well in 6-well plates (1 mL of medium per well). Cells were treated with DAC on day 1. Medium was changed every 2 days. Cells were split at 70% confluence with trypsin/EDTA, using standard protocols, followed by reseeding of the appropriate volume of cells. The cells used in these experiments were passaged 5 to 7 times.

Culture of other RCC cell lines

The RCC cell lines SK-RC-29, SK-RC-45, ACHN, and RENCA were cultured in RPMI 1640 with 10% FBS at 37°C in a humidified atmosphere with 5% CO_2 in air. SK-RC-29 and SK-RC-45 cell lines were gifts from Dr. N.H. Banker at The New York Hospital-Cornell Medical Center (19). The ACHN cell line was established in our laboratory (20). RENCA were purchased from American Type Culture Collection.

Derivation and culture of normal kidney epithelial cells

Kidney epithelial cells were isolated from surgical specimens obtained from patients undergoing nephrectomy for renal carcinoma. A 10-mm fragment of normal renal tissue was manually dissociated by mincing the fragment with scalpels while submerged in 10-mL medium in a 10-cm dish. Resultant cells were cultured in RPMI 1640 with 10% FBS at 37°C in a humidified atmosphere with 5% CO_2 in air. After cell expansion for 1 week, aliquots of primary cells were frozen in liquid nitrogen for later use. The kidney epithelial cells generated in this manner are nonimmortalized, nontumorigenic in nude mice and senesce after 20 to 30 passages.

Sequencing of TP53

PCR primers were designed to amplify all coding exons 3 to 11 and mRNA open reading frame sequence of *TP53* (NM_000546.4). Genomic DNA and first-strand cDNA were used as templates for PCR amplification. Bidirectional sequencing was done using ABI 3730xl DNA analyzer (Applied Biosystems). Primer sequences are given in Supplementary Table S1. Seqman software was used to analyze the sequences (DNASTAR)

In vitro treatment of cells with DAC

DAC stock solution (5 mmol/L) was generated by reconstituting lyophilized DAC in 100% methanol. Stock solution aliquots were stored at −80°C for up to 3 weeks. Working solution was generated by diluting the stock solution 1:100 in PBS, immediately before addition to the cells at a further dilution as per the intended final concentration. Similar amounts of methanol are added to untreated control cells. Cells were treated with DAC (0.5 μmol/L) on days 1, 4, and 7 of culture.

Immunofluorescence to measure DNMT1 levels and examine nuclear chromatin

Cells on cytospin slides were fixed and permeabilized with 10% formalin and 0.25% triton. Nonspecific binding sites were blocked with 10% normal goat serum and 6% bovine serum albumin (BSA). Slides were incubated overnight with mouse anti-DNMT1 antibody (Abcam; catalogue no. ab13537, diluted 1:500 in blocking solution), followed by a 655-nm Quantum Dots-conjugated goat anti-mouse antibody (Invitrogen; catalogue no. Q11022MP, diluted 1:500). Finally, cells were stained with 3 μmol/L 4′,6-diamidino-2-phenylindole (DAPI) for 5 minutes before dehydration in graded alcohols and xylene.

DNA damage measurement by γH2AX staining

Phosphorylation of the histone H2A family member H2AX at Ser139 (γH2AX) was measured by flow cytometry. Cells were fixed with 2% paraformaldehyde and then permeabilized by adding ice-cold 90% methanol solution. Cells were then incubated in blocking solution (0.5% BSA) containing saturating concentration of Alexa 488–conjugated γH2AX antibody (Cell Signaling Technology; catalogue no. 9719). Percentage of γH2AX-positive cells is analyzed with a Coulter Epics XL-MCL flow cytometer equipped with CXP software (Beckman-Coulter).

Apoptosis detection

Apoptosis was detected by Annexin-V and 7AAD costaining, using the APOAF commercial kit (Sigma). Cells (5×10^5), were washed and incubated for 30 minutes with fluorescein isothiocyanate–conjugated Annexin-V at room temperature. Cells were then resuspended in 400 mL of binding buffer containing 7AAD and immediately analyzed by flow cytometry.

PKH67 methods

PKH67 staining was carried out following the labeling procedure provided by the manufacturer (Sigma). Briefly, 10^7 cells were detached with 0.25% trypsin, washed once with RPMI 1640/10% FBS, and resuspended at the concentration of 2×10^7/mL in diluent C. The cell suspension was gently mixed with 1 mL of a 20 μmol/L PKH67 solution and incubated for

Downloaded from cancerres.aacrjournals.org on July 24, 2018. © 2011 American Association for Cancer Research.

Published OnlineFirst February 8, 2011; DOI: 10.1158/0008-5472.CAN-10-2422

3 minutes at room temperature. Staining was stopped by the addition of an equal volume (2 mL) of RPMI 1640/1% BSA for 1 minute. To remove the excessive dye, cells were washed 3 times and then either analyzed by flow cytometry (day 0) or replated in RPMI 1640/10% FBS for further analysis at indicated times (days 1, 2, and 3).

Quantitative real-time PCR

mRNA levels were assayed by quantitative real-time PCR (qRT-PCR) by standard methods. Glyceraldehyde 3-phosphate dehydrogenase was amplified as control. Primer sequences are given in Supplementary Table S1. Real-time detection of the emission intensity of SYBR Green bound to double-stranded DNA was detected using the iCycler instrument (Bio-Rad). Data were reported as "relative expression value," which was determined by raising 2 to the power of the negative value of $\Delta\Delta C_T$ for each sample.

One-dimensional SDS-PAGE and Western blotting

Approximately 50 μg of protein extracts, together with molecular weight markers, was subjected to one-dimensional (1D) SDS-PAGE on 4% to 12% gradient gels (Invitrogen). After electrophoresis per manufacturer's manual (Invitrogen), proteins were transferred to polyvinylidene difluoride (PVDF) membranes (Millipore) at 35 constant voltage for 1 hour, using Invitrogen's semidry blotting apparatus. Western analyses of PVDF membranes utilized established protocols and antibodies for p15 (Cell Signaling; catalogue no. 4822), p21 (Cell Signaling; catalogue no. 2946), p27 (Cell Signaling; catalogue no. 3686), p57 (Cell Signaling; catalogue no. 2557), p-p53 (Cell Signaling; catalogue no. 92865), p53 (Sigma-Aldrich; catalogue no. P6874), DNMT1 (Abcam; catalogue no. Ab54759), and anti–β-actin peroxidase (Sigma-Aldrich; catalogue no. A3854).

Murine xenograft and *in vivo* therapy with DAC

All experiments were approved by the Cleveland Clinic Institution Animal Care and Use Committee (IACUC) and followed approved procedures. Nude mice were inoculated subcutaneously (right and left flanks) with 1×10^6 Ren-01 cells in 200-μL sterile vehicle. Nine days after inoculation (day 9), mice were initiated on treatment (4 mice each per treatment group) with 0.2 mg/kg DAC administered subcutaneously 3 days per week, sunitinib [a multi-kinase (including VEGF pathway) inhibitor that is standard of care for metastatic RCC] 40 mg/kg administered by oral gavage daily 5 days per week, the combination of DAC and sunitinib, or mock treated with PBS administered subcutaneously. Size of the xenograft was recorded twice a week with an electronic caliper, and volume was estimated using the following equation: volume (mm^3) = long (mm) × wide (mm^2)/2. Mice developing tumors of more than 2,000 mm^3 in size or showing signs of distress or necropsy in any area of the xenograft were euthanized for humanitarian reasons, using CO_2 inhalation and followed by cervical dislocation. Tumor was harvested from the euthanized rodents for further analysis. The experiment was terminated when the mice from any experimental group were completely euthanized. Similar procedures were followed for experiments using RENCA, with the following differences: the inoculum consisted of 3×10^6 RENCA cells. DAC treatment was initiated 3 days after the inoculation with tumor cells. Sunitinib was not used a treatment regimen.

Correlation of KI67 gene expression with GI_{50}

Quality controlled raw data (Affymetrix CEL files or SOFT files) from previously published experiments [Gene Expression Omnibus (GEO) Datasets GSE5846; ref. 21] were downloaded from GEO datasets (www.ncbi.nlm.nih.gov/geo). KI67 gene expression data in 8 renal cancer cell lines (786-0, A498, ACHN, CAKI-1, RXF 393, SN12C, TK-10, and UO-31) were correlated with GI_{50} (the concentration of DAC that produced 50% growth inhibition) data from the Developmental Therapeutics Program of the National Cancer Institute (NCI; http://dtp.nci.nih.gov/index.html; ref. 22). SAS statistical analysis software was used to generate scatter plots and Spearman and Pearson correlation coefficients.

Cytospin and Giemsa staining

For morphology evaluation, the renal cancer cell lines were treated with 0.5 μmol/L DAC at day 1 and day 4 and harvested at day 7. Slides were spun down onto slides with a Shandon CytoSpin III cytocentrifuge (Thermo Scientific) at 500 rpm for 5 minutes. After air drying, cells were fixed with 100% methanol for 1 minute and then Giemsa stained: Giemsa staining stock solution was diluted with PBS (pH 6.5) at a ratio of 1:10, and the diluted Giemsa solution was added to cells for 30 minutes at room temperature. After rinsing and mounting of cover-slips, cell morphology was evaluated using an Olympus light microscope and CCD camera.

PCR and pyrosequencing assay for LINE-1 methylation

Genomic DNA was isolated from RENCA tumor explants with the Wizard Genomic DNA Purification kit (Promega; catalogue no. A1125) according to the manufacturer's protocol. Bisulfite conversion of the genomic DNA was done using the EZ DNA Methylation kit (Zymo Research; catalogue no. D5001) according to the manufacturer's protocols. Murine LINE-1 CpG methylation status was determined by pyrosequencing on the Qiagen PyroMark Q24 using PyroMark Gold Q24 reagents (Qiagen) according to the manufacturer's protocol. Sequence and methylation status analyses were done using the PyroMark Q24 version 1.0.10 software in the CpG (methylation) analysis mode. mouse LINE-1 forward primer: TGGGATTTTAAGATTTTTGGTGAG; reverse primer: CTTCCCTATTTACCACAATCTCAA (amplicon size 86 bp), annealing temperature: 60°C. Sequencing primer: TTTTTGGTGAGTGGAATATA (23). The amount of C divided by the sum of the amounts of C and T at each CpG site was calculated as percentage (i.e., multiplied by 100).

Statistical analysis

Student's *t* test was used to compare mean cell counts and relative expression values. Statistical comparisons involving more than 2 groups were carried out by 1-way ANOVA, with Dunnett multiple comparisons as *post hoc* test. Differences were considered statistically significant when $P < 0.05$.

Downloaded from cancerres.aacrjournals.org on July 24, 2018. © 2011 American Association for Cancer Research.

Published OnlineFirst February 8, 2011; DOI: 10.1158/0008-5472.CAN-10-2422

Results

DAC (0.5 μmol/L) depletes DNMT1 in Ren-01 cells without causing measurable DNA damage, apoptosis, or senescence

DAC is a cytosine analogue; therefore, as per the class effect of nucleoside analogues, it can induce DNA damage and cytotoxicity. However, the sugar backbone of DAC is unmodified, and DAC is rapidly cleaved and degraded by hydrolysis (24). Hence, DAC is substantially less efficient at impeding DNA replication machinery and terminating DNA strand elongation than an equimolar concentration of cytosine arabinoside (AraC), a cytosine analogue with prominent cytotoxic effects (8, 9). Here, to support a noncytotoxic DNMT1 depletion-based (and hence epigenetic) mechanism of action when low concentrations of DAC are used, we evaluated DNMT1 depletion, DNA damage, apoptosis, and senescence induction in RCC cells treated with DAC. Equimolar concentrations of the DNA-damaging cytosine analogue cytarabine (AraC) was used as a control in these experiments, because DAC and AraC are transported into cells and metabolized identically to generate nucleotide analogues that can incorporate into DNA.

DNMT1 was quantified in Ren-01 cells 48 hours after treatment with 0.5 μmol/L DAC. This concentration of DAC produced a substantial decrease in DNMT1 levels (Fig. 1A). Twenty-four hours after equimolar DAC or AraC treatment, cells were harvested for flow cytometric measurement of phospho-H2AX levels as an index of DNA damage/repair. AraC produced a large increase in phospho-H2AX levels (Fig. 1B). In contrast, equimolar DAC did not significantly increase phospho-H2AX levels (Fig. 1B). Apoptosis is associated with cell surface staining with Annexin-V. AraC treatment increased Annexin-V staining of Ren-01 cells (measured by flow cytometry 24 hours after drug treatment; Fig. 1C). In contrast, DAC-treated cells did not show an increase in Annexin-V staining (Fig. 1C). Another mechanism for cell-cycle exit is senescence, which is associated with distinctive patterns of chromatin clumping (25). DAC treatment of normal human fibroblasts induced chromatin changes associated with senescence

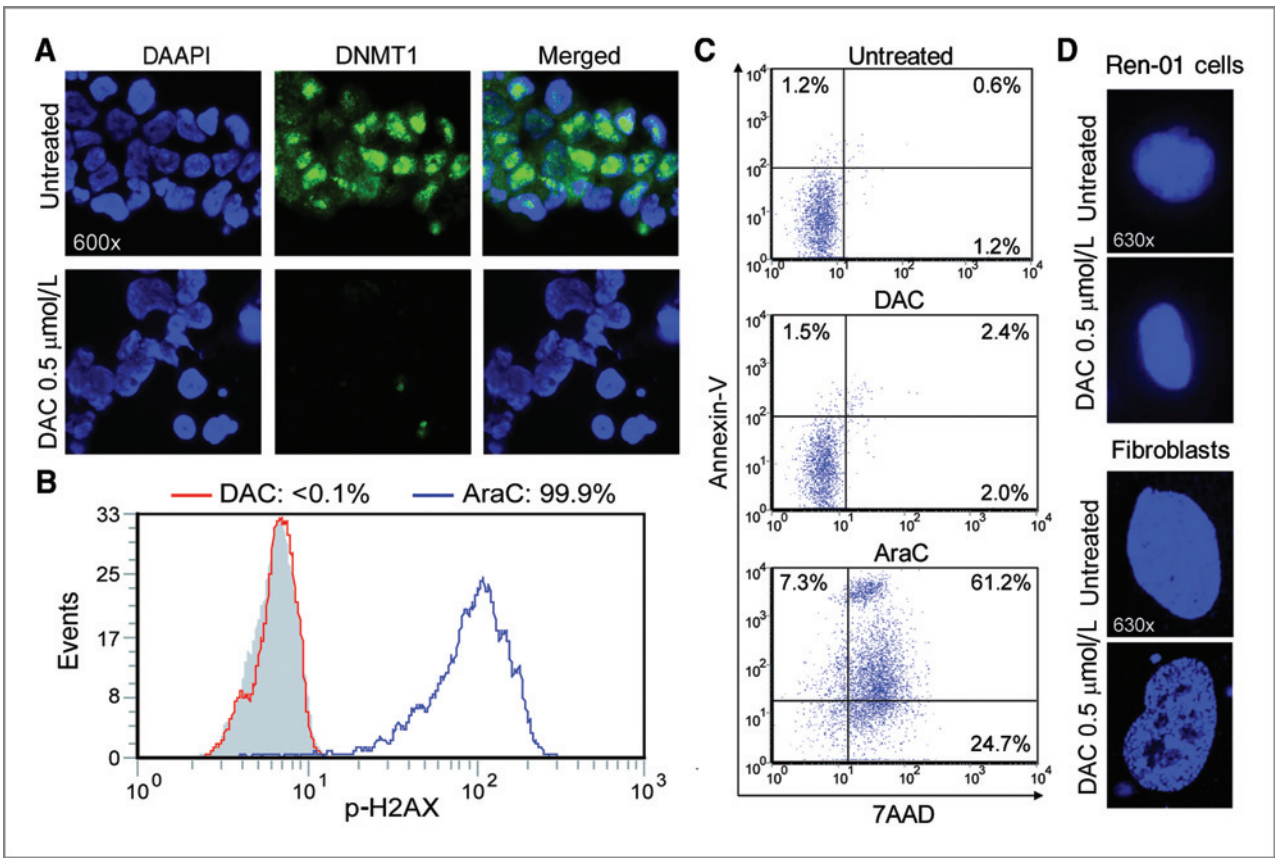

Figure 1. Administration of 0.5 μmol/L DAC depletes DNMT1 in Ren-01 cells without causing significant DNA damage or apoptosis. A, DNMT1 depletion in Ren-01 cells treated with 0.5 μmol/L DAC. Ren-01 cells (low passage number RCC cells) at less than 40% confluence were treated with 0.5 μmol/L DAC. DNMT1 was quantified 48 hours later by immunofluorescence (green dots). DAPI was used to stain nuclei (blue stain). B, this concentration did not produce measurable DNA damage in Ren-01 cells. Twenty-four hours after DAC or AraC exposure, DNA damage was measured by flow cytometric assessment for phosphorylation of histone H2AX. Equimolar levels of AraC were used as positive control. Grey histogram, isotype control. C, 0.5 μmol/L DAC did not produce early apoptosis in Ren-01 cells. Twenty-four hours after the addition of 0.5 μmol/L DAC or AraC, apoptosis was measured by flow cytometric assessment for Annexin-V/7AAD staining of exposed phosphatidyl serine. D, DAC produced chromatin changes associated with senescence in normal fibroblasts but not in Ren-01 cells. Normal human fibroblasts, but not Ren-01 cells, treated with DAC undergo clumping changes in chromatin associated with senescence (25).

Downloaded from cancerres.aacrjournals.org on July 24, 2018. © 2011 American Association for Cancer Research.

Published OnlineFirst February 8, 2011; DOI: 10.1158/0008-5472.CAN-10-2422

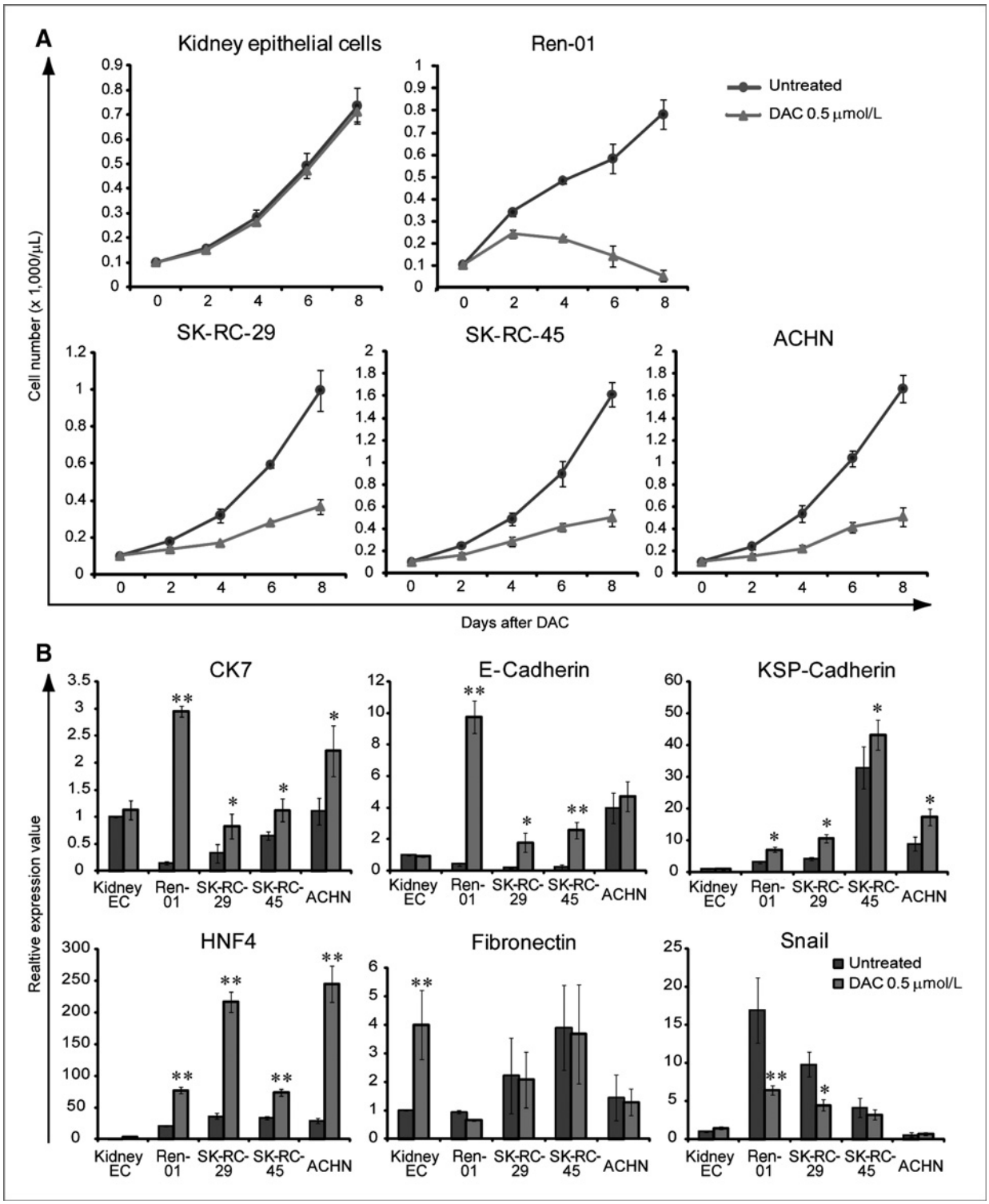

Figure 2. Noncytotoxic concentrations of DAC decreased proliferation of RCC cells accompanied by gene and protein expression changes of epithelial and terminal differentiation. A, normal kidney epithelial cells (EC) treated with DAC continued to proliferate similar to vehicle-treated control; in contrast, DAC treatment decreased the rate of proliferation in Ren-01 and the other RCC cell lines. Cells were treated *in vitro* with 0.5 μmol/L DAC on days 1 and 4 or mock-treated with PBS. Cells were counted by automated cell counter. Data points, mean cell count ± standard error. B, DAC treatment produced gene expression changes of epithelial differentiation in the RCC cell lines but not in normal kidney epithelial cells. mRNA expression measured by qRT-PCR 24 hours after DAC treatment unless otherwise specified. HNF4α, driver of kidney mesenchymal to epithelial transition. Fibronectin and Snail are mesenchymal markers. CK7, E-cadherin, and KSP-cadherin are epithelial markers. Dark grey bars, untreated control. Light grey bars, DAC-treated cells. Data points, mean expression value ± standard error. *, $P < 0.05$; **, $P < 0.01$ (*t* test).

Downloaded from cancerres.aacrjournals.org on July 24, 2018. © 2011 American Association for Cancer Research.

Published OnlineFirst February 8, 2011; DOI: 10.1158/0008-5472.CAN-10-2422

(Fig. 1D). These chromatin changes were not seen in Ren-01 cells treated with DAC (Fig. 1D).

DAC, at concentrations that depleted DNMT1 without causing measurable DNA damage or apoptosis, decreased proliferation of RCC cells accompanied by gene and protein expression changes of epithelial and terminal differentiation

Gene expression and pathomorphologic observations suggest that RCC cells may have an abnormal mesenchymal differentiation level (26–28). One potential mechanism of action by which chromatin-relaxing drugs may terminate proliferation of renal cancer cells is through restoration of more normal differentiation patterns, which would be expected to be accompanied by a decrease in mesenchymal markers and an increase in epithelial markers.

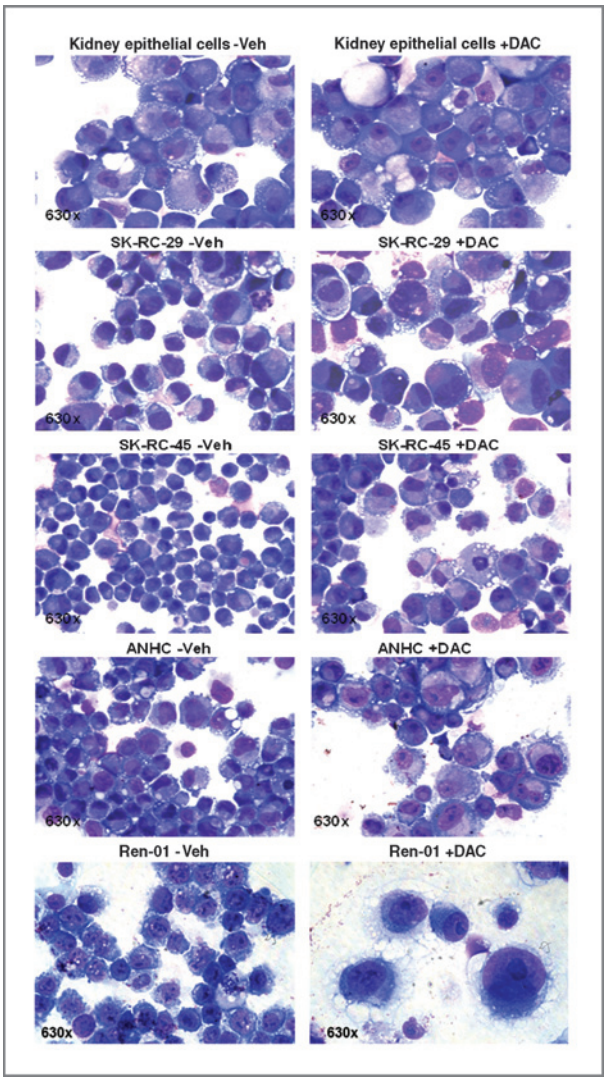

Figure 3. Morphology of normal kidney epithelial cells and RCC cell lines treated with vehicle or DAC. Vehicle (Veh) or 0.5 μmol/L DAC was added on day 1 and day 4; cells were harvested and stained with Giemsa on day 7.

Early-passage normal kidney epithelial cells, the freshly derived RCC cell line Ren-01 [a p53 mutated (Supplementary Fig. S1) cell line derived from a patient with treatment refractory RCC], and the established RCC cell lines SK-RC-29, SK-RC-45, and ACHN were either treated with the concentration of DAC that depleted DNMT1 without causing measurable apoptosis on days 1 and 4 or mock treated with PBS. Normal kidney epithelial cells treated with DAC continued to proliferate in a manner similar to the vehicle-treated control (Fig. 2A). In contrast, DAC treatment decreased the rate of proliferation in the RCC cell lines (Fig. 2A).

In the normal kidney epithelial cells (Fig. 2B), DAC treatment did not produce a significant change in the gene expression of hepatocyte nuclear factor 4α (HNF4α), a key DNA-binding transcription factor associated with mesenchymal to epithelial transition (29), or in the expression of the kidney epithelial markers cytokeratin 7 (CK7), epithelial cadherin (E-cadherin), and kidney-specific cadherin (KSP-cadherin). Expression of the mesenchymal marker fibronectin was increased, with a small increase in expression of the mesenchymal marker Snail (Fig. 2B). In contrast, in the RCC cell lines, DAC treatment increased expression of the mesenchymal to epithelial differentiation driver HNF4α, increased expression of the epithelial markers CK7, E-cadherin in 3 of 4 cell lines, and KSP-cadherin, and decreased expression of the mesenchymal markers Snail in 2 of 4 cell lines (Fig. 2B). The decrease in fibronectin levels was not statistically significant (Fig. 2B). Cells harvested on day 7 were stained with Giemsa to facilitate morphologic examination. Normal kidney epithelial cells treated with DAC resembled vehicle-treated cells. However, RCC cell lines (SK-RC-29, SK-RC-45, ANHC, and Ren-O1) treated with DAC showed increased size, decreased nucleocytoplasmic ratio, and increased eosinophilic staining of the cytoplasm compared with vehicle-treated cells (Fig. 3).

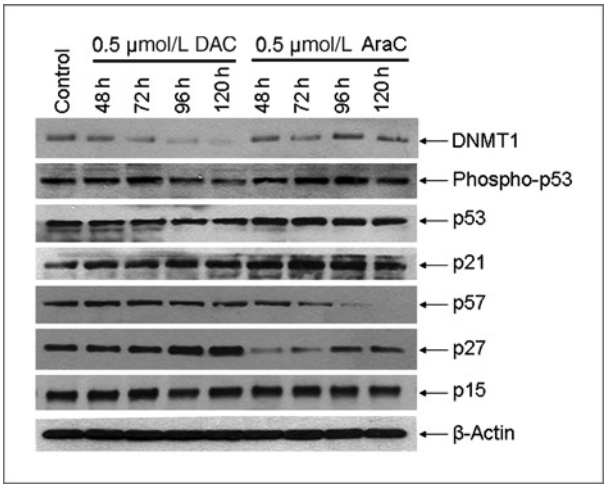

Figure 4. In Ren-01 cells, DAC but not AraC depleted DNMT1 and increased p27/CDKN1B protein levels at late time points. Protein levels measured by Western blot at the indicated time points. DAC or AraC (0.5 μmol/L) was added to the cells at 0 hour. Results with murine RCC cells (RENCA) are given in Supplementary Figure S2.

Downloaded from cancerres.aacrjournals.org on July 24, 2018. © 2011 American Association for Cancer Research.

Published OnlineFirst February 8, 2011; DOI: 10.1158/0008-5472.CAN-10-2422

The gene expression changes suggest that the decrease in proliferation in the RCC cell lines could be mediated by epithelial differentiation–associated cell-cycle exit. Key components of the apoptosis and differentiation pathways that mediate cell-cycle exit have been described. Apoptosis induced by antimetabolite chemotherapy is associated with the phosphorylation of p53 serine-15 and the upregulation of p53 and cyclin-dependent kinase inhibitors p21/CDKN1A and p16/CDKN2A (30–38). Differentiation–mediated cell-cycle exit is associated with the upregulation of p57/CDKN1C and p27/CDKN1B (39–42). Protein levels of these key mediators of apoptotic and differentiation cell-cycle exit were examined in Ren-01 cells at various time points (48–120 hours) after treatment with DAC or 0.5 μmol/L AraC.

With regard to apoptosis-associated events, AraC but not DAC produced a significant increase in serine-15 phosphorylation of p53 and levels of total p53 (Fig. 4). Both DAC and AraC increased p21/CDKN1A levels, with a larger increase produced by AraC (Fig. 4). p16/CDKN2A protein was not detected in Ren-01 cells despite using 2 separate antibody clones for detection (Fig. 4).

With regard to differentiation-associated events, only DAC but not AraC increased levels of p27/CDKN1B, with the increase most prominent at late time points (Fig. 4). AraC decreased p57/CDKN1C levels (Fig. 4). p57/CDKN1C levels were unaffected by DAC treatment (Fig. 4). Neither AraC nor DAC affected p15/CDKN2B levels (Fig. 4). DAC but not AraC decreased levels of DNMT1 (Fig. 4).

Levels of DNMT1 and the above-mentioned apoptosis and differentiation proteins were also examined in murine RCC cells (RENCA) treated with DAC or AraC. As per Ren-01, the most prominent observation was DNMT1 depletion and p27/CDKN1B upregulation at late time points in DAC-treated cells but not in AraC-treated cells (Supplementary Fig. S2A and B).

DAC-treated Ren-01 cells undergo temporary cell-cycle arrest and then resume cell division unlike AraC-treated cells which do not divide after treatment

The late upregulation of p27/CDKN1B suggests that cell-cycle exit after DAC treatment may be a late effect, with Ren-01 cells undergoing 1 or more cell divisions after DAC treatment before eventual differentiation–mediated cell-cycle exit unlike the immediate cell-cycle exit associated with apoptosis-based therapy.

Ren-01 cell membranes were stained with the fluorescent marker PHK67 prior to μmol/L DAC or AraC 0.5 treatment. This cell surface stain is diluted on the cell surface corresponding to the number of cell divisions. Compared with

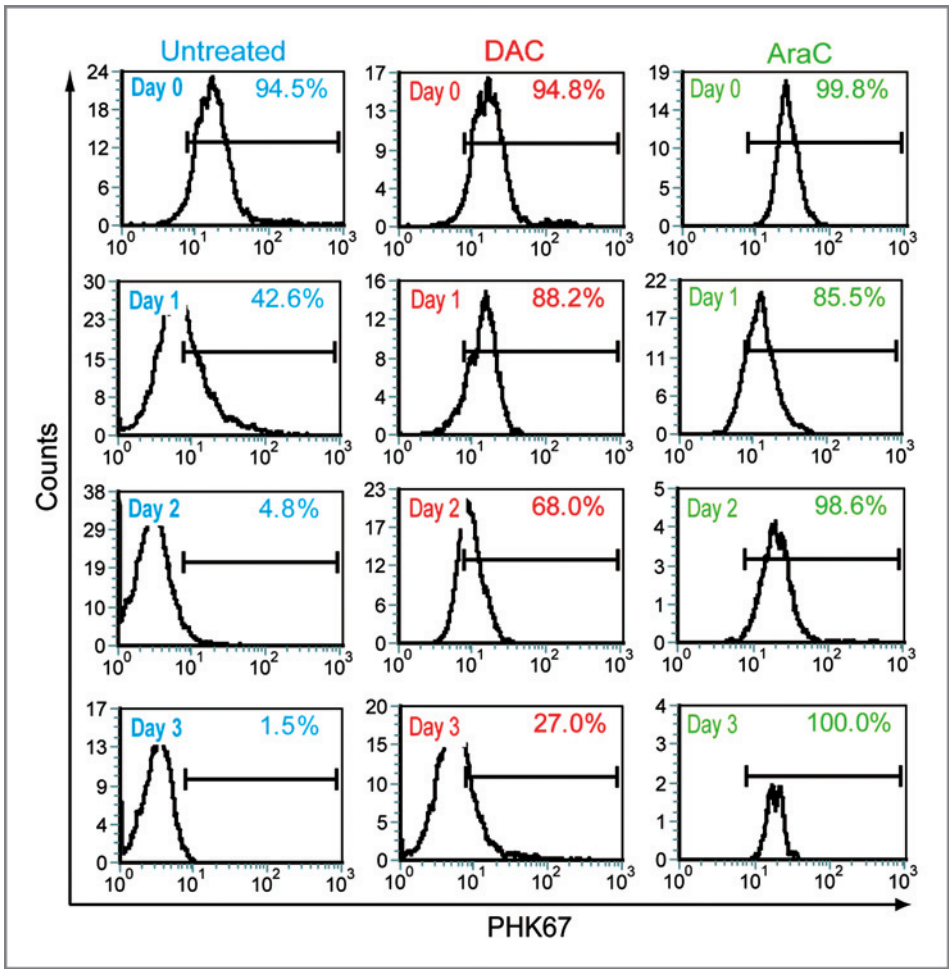

Figure 5. DAC-treated Ren-01 cells undergo temporary cell-cycle arrest and then resume cell division unlike AraC-treated cells which do not divide after treatment. Cell membranes were stained with PHK67 prior to DAC or AraC treatment. Left shift in signal corresponds to cell division with a consequent decrease in stain intensity on individual daughter cells. DAC and AraC treatment one-time addition of 0.5 μmol/L.

Downloaded from cancerres.aacrjournals.org on July 24, 2018. © 2011 American Association for Cancer Research.

Published OnlineFirst February 8, 2011; DOI: 10.1158/0008-5472.CAN-10-2422

PBS-treated control, DAC produced a temporary cell-cycle arrest, followed by a resumption in cell division (Fig. 5). In contrast, AraC induced cell-cycle arrest from which the Ren-01 cells did not recover (Fig. 5).

Sensitivity of renal cancer cell lines to DAC inversely correlates with the proliferative index

Because DAC is S-phase specific, sensitivity to DAC may depend on the proliferative index of RCC cells. In 8 RCC cell

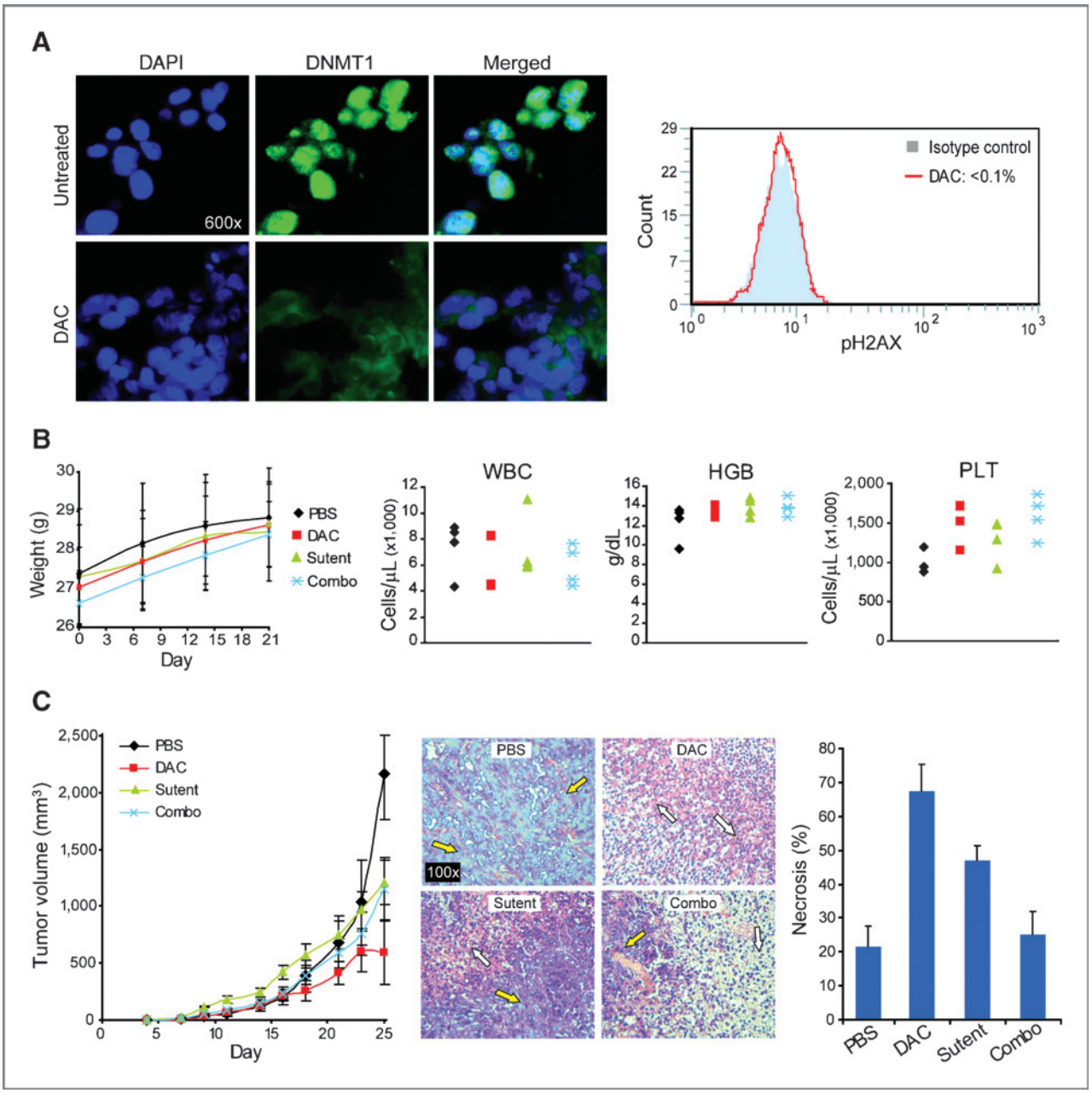

Figure 6. A noncytotoxic metronomic regimen of DAC (0.2 mg/kg s.c. 3 times per week) produced tumor regression *in vivo*. Nude mice were inoculated subcutaneously (right and left flanks) with 1×10^6 Ren-01 cells. Nine days after inoculation (day 9), mice were initiated on treatment (4 mice per treatment group) with 0.2 mg/kg DAC administered subcutaneously 3 times per week, sunitinib 40 mg/kg administered by oral gavage daily 5 times per week, the combination (combo) of DAC and sunitinib (Sutent), or mock-treated with PBS administered subcutaneously. A, DNMT1 depletion in Ren-01 explants without measurable bone marrow DNA damage. DNMT1 levels measured by immunofluorescence (green dots) analysis of tumor explant. DAPI (blue stain) of nuclei. DNA damage measured by phospho-H2AX staining of bone marrow aspirate cells in DAC-treated mice. B, this regimen of DAC was well tolerated, with no significant weight loss and stable blood counts. Blood counts by Hemavet. WBC, white blood cell; HGB, hemoglobin; PLT, platelet. C, DAC decreased tumor volume and increased tumor necrosis. Tumor necrosis was estimated in blinded fashion from hematoxylin and eosin staining of paraffin-embedded tumor explants. White arrows, areas of necrosis. Yellow arrows, areas of intact tumor tissue.

Downloaded from cancerres.aacrjournals.org on July 24, 2018. © 2011 American Association for Cancer Research.

Published OnlineFirst February 8, 2011; DOI: 10.1158/0008-5472.CAN-10-2422

lines (786-0, A498, ACHN, CAKI-1, RXF 393, SN12C, TK-10, and UO-31), the DAC GI_{50} [GI_{50} data from the Developmental Therapeutics Program of the NCI (http://dtp.nci.nih.gov/index.html) and gene expression data from GEO data sets GSE5846; ref. 21] inversely correlated with the expression of KI67 (a proliferation marker expressed only in cycling cells; KI67 expression is widely used in clinical pathology as an index of proliferation in tumor tissue; ref. 22; Supplementary Fig. S3).

A noncytotoxic dose and schedule of DAC was well tolerated and decreased tumor volume in xenografted mice

The *in vitro* observations suggest that a DAC dose intended for noncytotoxic DNMT1 depletion could be efficacious therapy. The sensitivity of DAC to the proliferative index suggests the importance of maximizing time of exposure (to increase the fraction of cancer cells that undergo cell division in the presence of DAC). The lower dose of DAC used for noncytotoxic DNMT1 depletion may allow relatively frequent administration to increase time of exposure (3 times per week). Although low-dose DAC can be noncytotoxic, temporary cell-cycle arrest (cytostasis) is likely still produced. Daily administration could prolong cytostasis and thereby cause or exacerbate cytopenia. Nondaily, but relatively frequent, 1 to 3 times per week, administration is a stratagem to maximize cumulative exposure while minimizing consequences of cytostasis such as cytopenia. Similarly, subcutaneous administration may produce lower peak levels but extend the duration of exposure compared with intraperitoneal administration of DAC. These principles were tested using a xenograft model of human RCC.

Nude mice were inoculated subcutaneously (right and left flanks) with 1×10^6 Ren-01 cells. Nine days after inoculation, mice were initiated on treatment with 0.2 mg/kg DAC administered subcutaneously 3 times per week, sunitinib [a multikinase (including VEGF pathway) inhibitor that is a standard of care for metastatic RCC] 40 mg/kg administered by oral gavage daily 5 times per week, the combination of DAC and sunitinib, or mock treated with PBS administered subcutaneously (4 mice each per treatment group).

This regimen of DAC did not induce measurable DNA damage in the bone marrow of DAC-treated mice (measured by flow cytometric assessment of phospho-H2AX levels; Fig. 6A). Murine weights in DAC- and sunitinib-treated mice were similar and decreased, but not to significant extent, compared with PBS-treated mice. The largest decrease in murine weights was seen in mice treated with the combination of DAC and sunitinib (Fig. 6B). No substantial differences in white blood cell, platelet, or hemoglobin levels were noted between the different treatment groups, although there was a trend toward higher platelet counts in mice receiving DAC (Fig. 6B, increases in platelet counts are noted with low-dose DAC clinical therapy; ref. 10). The greatest decrease in tumor volume was produced by treatment with DAC (Fig. 6C). On day 25 (after 2 weeks of treatment), the tumor volume in DAC, sunitinib, and combination treated mice was significantly decreased compared with PBS-treated control mice (P values 0.003, 0.028, and 0.048, respectively). Tumor explants were fixed and embedded in paraffin and evaluated histologically by hematoxylin and eosin staining. DAC treatment was associated with more extensive necrosis than treatment with sunitinib or the combination (Fig. 6C).

The DAC regimen produced similar results when a different RCC cell line was used: nude mice were inoculated subcutaneously with 3×10^6 RENCA cells. Subcutaneous administration of 0.2 mg/kg DAC 3 times per week or PBS mock treatment was initiated on day 3. In vehicle-treated mice, there was an exponential increase in tumor volume requiring early sacrifice of the mice (Supplementary Fig. S2C). In DAC-treated mice, there was a substantially slower early increase in tumor volume, followed by no further tumor growth (Supplementary Fig. S2C). In a parallel experiment, RENCA tumor was explanted on day 21 from 2 vehicle and 2 DAC-treated mice for evaluation of tumor DNMT1 by Western blot and DNA methylation by LINE-1 pyrosequencing. Compared with explants from vehicle-treated mice, DNMT1 and DNA methylation levels were substantially decreased in explants from DAC-treated mice (Supplementary Fig. S2D).

Discussion

Both Wilms' and non-Wilms' tumor renal cancer cells have gene expression profiles, with features of mesenchymal differentiation instead of normal epithelial differentiation (26–28). This suggests an RCC model in which the self-renewal that drives expansion of the malignant clone derives from abnormal persistence, or acquisition of, an immature mesenchymal program (reviewed in ref. 43). A corollary of this model is abnormal repression of the epithelial differentiation program. Repression of the epithelial differentiation program could be mediated epigenetically, even if genetic events are the upstream triggers for abnormal differentiation. Supporting a role for aberrant epigenetic repression in RCC oncogenesis, mutations in chromatin-modifying enzymes that create epigenetic activation marks are a feature of RCC (44). The observations here, in which noncytotoxic DNMT1 depleting concentrations of DAC increased epithelial marker expression, decreased mesenchymal marker expression and increased expression of p27/CDKN1B protein, the CDKN family member with a well-documented role in mediating cell-cycle exit with differentiation (39–42), are consistent with this model of RCC oncogenesis.

This noncytotoxic epigenetic approach to therapy could complement existing therapy in a number of ways. Noncytotoxic DNMT1 depletion with DAC increases normal hematopoietic stem cell self-renewal and is well tolerated, even in subjects with comorbidities (10, 13–16, 45). The mechanism of action is likely to be distinct from current VEGF- and mTOR-targeted therapies. Rapamycin-induced cell-cycle exit was intact in $p27^{-/-}$ cells (41). This suggests that mTOR-targeted therapy and noncytotoxic DNMT1 depletion could be antiproliferative via different pathways. Moreover, the absence of early apoptosis, and the protein expression changes noted with DAC treatment of the p53-mutated RCC cell line, suggests that differentiation-mediated cell-cycle exit may be

Downloaded from cancerres.aacrjournals.org on July 24, 2018. © 2011 American Association for Cancer Research.

Published OnlineFirst February 8, 2011; DOI: 10.1158/0008-5472.CAN-10-2422

independent of p53/apoptosis pathways that are frequently mutated or attenuated in malignant cells.

DAC was originally developed as a DNA-damaging cytotoxic agent (46). Therefore, in traditional phase 1 studies, doses were escalated to maximum tolerated levels. In 14 RCC patients treated with pulse-cycled cytotoxic DAC (75 mg/m^2 administered intravenously for >1 hour every 7 hours for 3 doses, with cycles repeated every 5 weeks), there was no antitumor activity (47). Rationalizing the pharmacodynamic objective of therapy from cytotoxicity to noncytotoxic DNMT1 depletion enables lowering of the dose to approximately 7.5 mg/m^2 (10), because DNMT1 depletion can be achieved with relatively low concentrations of DAC. The resulting decrease in toxicity can enable more frequent administration to increase the time of exposure, a critical consideration with S-phase–specific therapy (because increasing time of exposure will facilitate incorporation of drug into a greater fraction of the tumor cell population). S-phase dependence of DAC could be a likely explanation for the decrease in efficacy observed with concurrent sunitinib (sunitinib may have had cytostatic effects on the RCC cells).

DAC has been investigated as a possible adjunct to immunotherapy to reactivate expression of genes that could favor immune recognition and destruction of tumor (4, 12). In a clinical trial examining the combination of DAC and interleukin-2 to treat RCC and melanoma (12), the dose of DAC was reduced to levels that are noncytotoxic when administered 1 to 3 times per week (10). However, daily administration of this dose, 5 days per week in weeks 1 and 2 of the 12-week cycles in this trial, contributed to significant leukopenia. Although low-dose DAC can be noncytotoxic, temporary cell-cycle arrest (cytostasis) is likely still produced. Therefore, daily DAC administration could prolong cytostasis and cause or exacerbate cytopenia. The nondaily, but relatively frequent, 3 times per week administration used in the xenograft model here was a stratagem to maximize cumulative exposure while minimizing consequences of cytostasis such as cytopenia. This type of DAC dose and schedule has been used to treat nonmalignant disease (10). A major side effect was an increase in platelet counts during therapy, indicating minimal cytostatic/cytotoxic effects (10). As shown here, extended cytostasis is not required for differentiation therapy of RCC. Indeed, the late increase in p27 expression (peaking at day 5 after DAC treatment), the late reduction in cell proliferation and tumor xenograft size, and the observation that DAC-treated RCC cells can resume cell division (by days 2–3) suggest that differentiation-mediated RCC cell-cycle exit may occur after 1 to 2 cell divisions. The present *in vitro* and *in vivo* results suggest that noncytotoxic regimens similar to those used in nonmalignant disease merit clinical study in RCC; however, responses may be more gradual than with conventional cytostatic/cytotoxic therapy.

The observations here provide *in vitro* and *in vivo* support for rationalizing dose and schedule of DAC for noncytotoxic epigenetic differentiation therapy of RCC. The differentiation-based mechanism of action spares normal stem cells, seems not to depend on p53/apoptosis pathways, and facilitates greater exposure to therapy. This treatment, with a distinctive mechanism of action, could complement existing treatment options and warrants further preclinical and clinical investigation.

Disclosure of Potential Conflicts of Interest

No potential conflicts of interest were disclosed.

Acknowledgments

The authors thank Rebecca Haney for animal care assistance and Dr N.H. Banker at The New York Hospital-Cornell Medical Center for the RCC cell lines SK-RC-29 and SK-RC-45.

Grant Support

O. Alcazar and K.P. Ng are supported by Scott Hamilton CARES. Y. Saunthararajah is supported by NIH (1R01CA138858, U54HL090513) and Department of Defense (PR081404).

The costs of publication of this article were defrayed in part by the payment of page charges. This article must therefore be hereby marked *advertisement* in accordance with 18 U.S.C. Section 1734 solely to indicate this fact.

Received July 7, 2010; revised November 30, 2010; accepted December 13, 2010; published OnlineFirst February 8, 2011.

References

1. Rini BI, Atkins MB. Resistance to targeted therapy in renal-cell carcinoma. Lancet Oncol 2009;10:992–1000.
2. Hagiwara H, Sato H, Ohde Y, Takano Y, Seki T, Ariga T, et al. 5-Aza-2′-deoxycytidine suppresses human renal carcinoma cell growth in a xenograft model via up-regulation of the connexin 32 gene. Br J Pharmacol 2008;153:1373–81.
3. Alleman WG, Tabios RL, Chandramouli GV, Aprelikova ON, Torres-Cabala C, Mendoza A, et al. The *in vitro* and *in vivo* effects of re-expressing methylated von Hippel-Lindau tumor suppressor gene in clear cell renal carcinoma with 5-aza-2′-deoxycytidine. Clin Cancer Res 2004;10:7011–21.
4. Coral S, Sigalotti L, Altomonte M, Engelsberg A, Colizzi F, Cattarossi I, et al. 5-Aza-2′-deoxycytidine-induced expression of functional cancer testis antigens in human renal cell carcinoma: immunotherapeutic implications. Clin Cancer Res 2002;8:2690–5.
5. Pili R. Recent investigations of histone deacetylase inhibitors in renal cell carcinoma. Clin Adv Hematol Oncol 2009;7:252–4.
6. Tuma RS. Epigenetic therapies move into new territory, but how exactly do they work?J Natl Cancer Inst 2009;101:1300–1.
7. Haaf T. The effects of 5-azacytidine and 5-azadeoxycytidine on chromosome structure and function: implications for methylation-associated cellular processes. Pharmacol Ther 1995;65:19–46.
8. Covey JM, D'Incalci M, Tilchen EJ, Zaharko DS, Kohn KW. Differences in DNA damage produced by incorporation of 5-aza-2′-deoxycytidine or 5,6-dihydro-5-azacytidine into DNA of mammalian cells. Cancer Res 1986;46:5511–7.
9. Schermelleh L, Haemmer A, Spada F, Rosing N, Meilinger D, Rothbauer U, et al. Dynamics of Dnmt1 interaction with the replication machinery and its role in postreplicative maintenance of DNA methylation. Nucleic Acids Res 2007;35:4301–2.
10. Saunthararajah Y, Hillery CA, Lavelle D, Molokie R, Dorn L, Bressler L, et al. Effects of 5-aza-2′-deoxycytidine on fetal hemoglobin levels, red cell adhesion, and hematopoietic differentiation in patients with sickle cell disease. Blood 2003;102:3865–70.

Downloaded from cancerres.aacrjournals.org on July 24, 2018. © 2011 American Association for Cancer Research.

Published OnlineFirst February 8, 2011; DOI: 10.1158/0008-5472.CAN-10-2422

11. Halaban R, Krauthammer M, Pelizzola M, Cheng E, Kovacs D, Sznol M, et al. Integrative analysis of epigenetic modulation in melanoma cell response to decitabine: clinical implications. PLoS One 2009;4:e4563.
12. Gollob JA, Sciambi CJ, Peterson BL, Richmond T, Thoreson M, Moran K, et al. Phase I trial of sequential low-dose 5-aza-2′-deoxycytidine plus high-dose intravenous bolus interleukin-2 in patients with melanoma or renal cell carcinoma. Clin Cancer Res 2006;12:4619–27.
13. Milhem M, Mahmud N, Lavelle D, Araki H, Desimone J, Saunthararajah Y, et al. Modification of hematopoietic stem cell fate by 5-aza-2′deoxycytidine and trichostatin A. Blood 2004;103:4102–10.
14. Chung YS, Kim HJ, Kim TM, Hong SH, Kwon KR, An S, et al. Undifferentiated hematopoietic cells are characterized by a genome-wide undermethylation dip around the transcription start site and a hierarchical epigenetic plasticityBlood 2009;114:4968–78.
15. Suzuki M, Harashima A, Okochi A, Yamamoto M, Nakamura S, Motoda R, et al. 5-Azacytidine supports the long-term repopulating activity of cord blood CD34(+) cells. Am J Hematol 2004;77:313–5.
16. Hu Z, Negrotto S, Gu X, Mahfouz R, Ng KP, Ebrahem Q, et al. Maintains hematopoietic precursor self-renewal by preventing repression of stem cell genes by a differentiation-inducing stimulus. Mol Cancer Ther 2010;9:1536–43.
17. Gurova KV, Hill JE, Razorenova OV, Chumakov PM, Gudkov AV. p53 pathway in renal cell carcinoma is repressed by a dominant mechanism. Cancer Res 2004;64:1951–8.
18. Roberts AM, Watson IR, Evans AJ, Foster DA, Irwin MS, Ohh M. Suppression of hypoxia-inducible factor 2alpha restores p53 activity via Hdm2 and reverses chemoresistance of renal carcinoma cells. Cancer Res 2009;69:9056–64.
19. Ebert T, Bander NH, Finstad CL, Ramsawak RD, Old LJ. Establishment and characterization of human renal cancer and normal kidney cell lines. Cancer Res 1990;50:5531–6.
20. Bauer JA, Morrison BH, Grane RW, Jacobs BS, Borden EC, Lindner DJ. IFN-alpha2b and thalidomide synergistically inhibit tumor-induced angiogenesis. J Interferon Cytokine Res 2003;23:3–10.
21. Lee JK, Havaleshko DM, Cho H, Weinstein JN, Kaldjian EP, Karpovich J, et al. A strategy for predicting the chemosensitivity of human cancers and its application to drug discovery. Proc Natl Acad Sci U S A 2007;104:13086–91.
22. Gerdes J, Schwab U, Lemke H, Stein H. Production of a mouse monoclonal antibody reactive with a human nuclear antigen associated with cell proliferation. Int J Cancer 1983;31:13–20.
23. Maegawa S, Hinkal G, Kim HS, Shen L, Zhang L, Zhang J, et al. Widespread and tissue specific age-related DNA methylation changes in mice. Genome Res 2010;20:332–40.
24. Rogstad DK, Herring JL, Theruvathu JA, Burdzy A, Perry CC, Neidigh JW, et al. Chemical decomposition of 5-aza-2'-deoxycytidine (decitabine): kinetic analyses and identification of products by NMR, HPLC, and mass spectrometry. Chem Res Toxicol 2009;22:1194–204.
25. Narita M, Nunez S, Heard E, Narita M, Lin AW, Hearn SA, et al. Rb-mediated heterochromatin formation and silencing of E2F target genes during cellular senescence. Cell 2003;113:703–16.
26. Tavares TS, Nanus D, Yang XJ, Gudas LJ. Gene microarray analysis of human renal cell carcinoma: the effects of HDAC inhibition and retinoid treatment. Cancer Biol Ther 2008;7:1607–18.
27. Hosono S, Luo X, Hyink DP, Schnapp LM, Wilson PD, Burrow CR, et al. WT1 expression induces features of renal epithelial differentiation in mesenchymal fibroblasts. Oncogene 1999;18:417–27.
28. Li CM, Guo M, Borczuk A, Powell CA, Wei M, Thaker HM, et al. Gene expression in Wilms' tumor mimics the earliest committed stage in the metanephric mesenchymal-epithelial transition. Am J Pathol 2002;160:2181–90.
29. Parviz F, Matullo C, Garrison WD, Savatski L, Adamson JW, Ning G, et al. Hepatocyte nuclear factor 4alpha controls the development of a hepatic epithelium and liver morphogenesis. Nat Genet 2003;34:292–6.
30. Wattel E, Preudhomme C, Hecquet B, Vanrumbeke M, Quesnel B, Dervite I, et al. p53 mutations are associated with resistance to chemotherapy and short survival in hematologic malignancies. Blood 1994;84:3148–57.
31. Stirewalt DL, Kopecky KJ, Meshinchi S, Appelbaum FR, Slovak ML, Willman CL, et al. FLT3, RAS, and TP53 mutations in elderly patients with acute myeloid leukemia. Blood 2001;97:3589–95.
32. Andersen MK, Christiansen DH, Kirchhoff M, Pedersen-Bjergaard J. Duplication or amplification of chromosome band 11q23, including the unrearranged MLL gene, is a recurrent abnormality in therapy-related MDS and AML, and is closely related to mutation of the TP53 gene and to previous therapy with alkylating agents. Genes Chromosomes Cancer 2001;31:33–41.
33. Schoch C, Kern W, Kohlmann A, Hiddemann W, Schnittger S, Haferlach T. Acute myeloid leukemia with a complex aberrant karyotype is a distinct biological entity characterized by genomic imbalances and a specific gene expression profile. Genes Chromosomes Cancer 2005;43:227–38.
34. Akashi K, He X, Chen J, Iwasaki H, Niu C, Steenhard B, et al. Transcriptional accessibility for genes of multiple tissues and hematopoietic lineages is hierarchically controlled during early hematopoiesis. Blood 2003;101:383–9.
35. Suarez L, Vidriales MB, Garcia-Larana J, Sanz G, Moreno MJ, Lopez A, et al. $CD34^+$ cells from acute myeloid leukemia, myelodysplastic syndromes, and normal bone marrow display different apoptosis and drug resistance-associated phenotypes. Clin Cancer Res 2004;10:7599–606.
36. Vazquez A, Bond EE, Levine AJ, Bond GL. The genetics of the p53 pathway, apoptosis and cancer therapy. Nat Rev Drug Discov 2008;7:979–87.
37. Kim WY, Sharpless NE. The regulation of INK4/ARF in cancer and aging. Cell 2006;127:265–75.
38. Gartel AL, Tyner AL. Transcriptional regulation of the p21((WAF1/CIP1)) gene. Exp Cell Res 1999;246:280–9.
39. Kiyokawa H, Kineman RD, Manova-Todorova KO, Soares VC, Hoffman ES, Ono M, et al. Enhanced growth of mice lacking the cyclin-dependent kinase inhibitor function of p27(Kip1). Cell 1996;85:721–32.
40. Fero ML, Rivkin M, Tasch M, Porter P, Carow CE, Firpo E, et al. A syndrome of multiorgan hyperplasia with features of gigantism, tumorigenesis, and female sterility in p27(Kip1)-deficient mice. Cell 1996;85:733–44.
41. Nakayama K, Ishida N, Shirane M, Inomata A, Inoue T, Shishido N, et al. Mice lacking p27(Kip1) display increased body size, multiple organ hyperplasia, retinal dysplasia, and pituitary tumors. Cell 1996;85:707–20.
42. Cheng T, Rodrigues N, Dombkowski D, Stier S, Scadden DT. Stem cell repopulation efficiency but not pool size is governed by p27(kip1). Nat Med 2000;6:1235–40.
43. Hay ED. An overview of epithelio-mesenchymal transformation. Acta Anat 1995;154:8–20.
44. Dalgliesh GL, Furge K, Greenman C, Chen L, Bignell G, Butler A, et al. Systematic sequencing of renal carcinoma reveals inactivation of histone modifying genes. Nature 2010;463:360–3.
45. Saunthararajah Y, Molokie R, Saraf S, Sidhwani S, Gowhari M, Vara S, et al. Clinical effectiveness of decitabine in severe sickle cell disease. Br J Haematol 2008;141:126–9.
46. Sorm F, Vesely J. Effect of 5-aza-2′-deoxycytidine against leukemic and hemopoietic tissues in AKR mice. Neoplasma 1968;15:339–43.
47. Abele R, Clavel M, Dodion P, Bruntsch U, Gundersen S, Smyth J, et al. The EORTC Early Clinical Trials Cooperative Group experience with 5-aza-2′-deoxycytidine (NSC 127716) in patients with colo-rectal, head and neck, renal carcinomas and malignant melanomas. Eur J Cancer Clin Oncol 1987;23:1921–4.

Downloaded from cancerres.aacrjournals.org on July 24, 2018. © 2011 American Association for Cancer Research.

Published OnlineFirst February 8, 2011; DOI: 10.1158/0008-5472.CAN-10-2422

Cancer Research
The Journal of Cancer Research (1916–1930) | The American Journal of Cancer (1931–1940)

AACR American Association for Cancer Research

Noncytotoxic Differentiation Treatment of Renal Cell Cancer

Soledad Negrotto, Zhenbo Hu, Oscar Alcazar, et al.

Cancer Res 2011;71:1431-1441. Published OnlineFirst February 8, 2011.

Updated version	Access the most recent version of this article at: doi:10.1158/0008-5472.CAN-10-2422
Supplementary Material	Access the most recent supplemental material at: http://cancerres.aacrjournals.org/content/suppl/2011/02/07/0008-5472.CAN-10-2422.DC1

Cited articles	This article cites 47 articles, 17 of which you can access for free at: http://cancerres.aacrjournals.org/content/71/4/1431.full#ref-list-1
Citing articles	This article has been cited by 2 HighWire-hosted articles. Access the articles at: http://cancerres.aacrjournals.org/content/71/4/1431.full#related-urls

E-mail alerts	Sign up to receive free email-alerts related to this article or journal.
Reprints and Subscriptions	To order reprints of this article or to subscribe to the journal, contact the AACR Publications Department at pubs@aacr.org.
Permissions	To request permission to re-use all or part of this article, use this link http://cancerres.aacrjournals.org/content/71/4/1431. Click on "Request Permissions" which will take you to the Copyright Clearance Center's (CCC) Rightslink site.

Downloaded from cancerres.aacrjournals.org on July 24, 2018. © 2011 American Association for Cancer Research.